Clim Dyn (2012) 39:2993–3005
DOI 10.1007/s00382-012-1414-0

On the fog variability over south Asia

F. S. Syed · H. Körnich · M. Tjernström

Received: 20 September 2011 / Accepted: 29 May 2012 / Published online: 21 June 2012
© Springer-Verlag 2012

Abstract An increasing trend in fog frequencies over south Asia during winter in the last few decades has resulted in large economical losses and has caused substantial difficulties in the daily lives of people. In order to better understand the fog phenomenon, we investigated the climatology, inter-annual variability and trends in the fog occurrence from 1976 to 2010 using observational data from 82 stations, well distributed over India and Pakistan. Fog blankets large area from Pakistan to Bangladesh across north India from west to east running almost parallel to south of the Himalayas. An EOF analysis revealed that the fog variability over the whole region is coupled and therefore must be governed by some large scale phenomenon on the inter-annual time scale. Significant positive trends were found in the fog frequency but this increase is not gradual, as with the humidity, but comprises of two distinct regimes shifts, in 1990 and 1998, with respect to both mean and variance. The fog is also detected in ERA-Interim 3 hourly, surface and model level forecast data when using the concept of "cross-over temperature" combined with boundary layer stability. This fog index is able to reproduce the regime shift around 1998 and shows that the method can be applied to analyze fog over south Asia. The inter-annual variability seems to be associated with the wave train originating from the North Atlantic in the upper troposphere that when causing higher pressure over the region results in an increased boundary layer stability and surface-near relative humidity. The trend and shifts in the fog occurrence seems to be associated with the gradual increasing trend in relative humidity from 1990 onwards.

Keywords Fog · South-Asia · Inter-annual variability · Trend · Fog detection

F. S. Syed (✉)
Department of Meteorology, Stockholm University,
10691 Stockholm, Sweden
e-mail: faisal@misu.su.se

F. S. Syed
Pakistan Meteorological Department,
44000 Islamabad, Pakistan

H. Körnich · M. Tjernström
Department of Meteorology, The Bert Bolin Centre
for Climate Research, Stockholm University,
10691 Stockholm, Sweden

1 Introduction

One of the major weather hazards in South Asian winter is heavy fog, which may extend over tens to thousands of kilometers and lasts for several days. Fog reduces visibility which results in accidents and also affects human health. The total economic loss associated with the impact of fog occurrence can be comparable to that of tornadoes or, in some cases, winter storms and hurricanes (Gultepe et al. 2007). As an example there were 217 flight diversions during January 2010 alone Delhi International Airport, with cancellations and delaying of thousands of flights as a consequence.

Over northern India, most of the fog formation is due to radiative cooling but, advection fog has also been observed (Dutta 2010). Radiation fog usually forms near the surface under clear skies in stagnant air in association with an anticyclone (Gultepe et al. 2007). The main mechanism is radiative cooling, but the opposing influences of upward soil heat flux, as well as warming effects and moisture losses through dew deposition and from turbulent mixing in the stable boundary layer largely determine the likelihood

and timing of radiation fog formation (Roach et al. 1976; Turton and Brown 1987; Fitzjarrald and Lala 1989; Duynkerke 1999). Radiation fog is more likely to occur when wind speed is low, relative humidity is high and surface temperature is low, so that the static stability is high (Sachweh and Koepke 1995; Niu et al. 2009). During such conditions mixing of air with the free troposphere is limited due to the trapping boundary-layer inversion. Such conditions ultimately result in poor visibility and high levels of pollutants in urban areas, since pollutants cannot be dispersed (Tiwari et al. 2010). The effect of urbanization and human activity on the fog formation is very complex. Collier (1970) mentioned that fog occurs more frequently in cities in comparison to airports which are usually away from the city urban air pollution. Landsberg (1964) also indicated that urban areas may experience a doubling of winter fog compared to adjacent rural areas. More persistent fogs in urban areas are attributed to air pollution effects, due to a large number of additional nuclei, expected to produce increased numbers of smaller fog droplets. The polluted cloud being capable of having eight times as many droplets of half the size, twice the surface area, twice the optical depth, thus can cause higher obscurity than natural clouds (Toon et al. 2000). Secondly the formation of fog droplets at sub-saturated conditions may occur in polluted air. Where decreasing concentrations of aerosols have been observed dense fog has also disappeared (Steve 2005). However, Sachweh and Koepke (1995) reported that an increase in urban building density is connected with a reduction in the average number of fog days, which they interpreted as an effect of the urban heat island and moisture deficit. Due to the thin and broken fog cover over urban environment, this radiative heating of the surface after sunrise may also lead to fog dissolution. Soil conditions also play an important role in radiation fog formation. Clay and silt loams, common soils found in the plains, have the ability to hold more moisture than sandy soils, because they are more porous and have a lower thermal conductivity (Rosenburg et al. 1983). This limits latent heat flux to the surface and allows radiative cooling to dominate and induce formation of surface inversions and fog.

However, accurate deterministic forecasts of fog need models and observations with a very high resolution and are not operationally feasible for a large domain and for longer forecasts (Stoelinga and Warner 1999; Tardif 2007; Burrows and Toth 2011). The most effective method for timely production of longer term forecasts of fog over large areas is a diagnostic approach (Zhou and Du 2010). Various diagnostic methods to produce forecasts of fog and stratus have been suggested over the years. The fog is diagnosed by local forecasters based either on statistical methods such as model output statistics (Koziara et al. 1983) and neural network (Fabbian et al. 2007; Marzban et al. 2007) or on indirect model output variables (e.g. Baker et al. 2002). With the increase in computer capacity, diagnostic approaches are now centered on making forecasts from numerical weather prediction (NWP) model output, using physically-based rules (e.g. Baker et al. 2002; Zhou and Du 2010; Marzban et al. 2007). Zhou and Du (2010) proposed a multivariable-based diagnostic fog-forecasting method based on five basic model variables: lowest model level liquid water content (LWC), cloud top, cloud base, 10-m wind speed, and 2-m relative humidity. Burrows and Toth (2011) implemented the method of Baker et al. (2002) for fog detection over Canada, making modifications and enhancements in the method to detect fog from numerical weather prediction model data. Baker et al. (2002) supplemented their technique by computing the so-called Modified Richardson number (MRi) to account for the effects of turbulence. The role of turbulence in the evolution of radiation fog remains controversial (Terradellas et al. 2008). Roach et al. (1976) stated that turbulence is a factor that inhibits the onset of radiation fog, others (e.g. Welch and Welicki 1986) support the theory that turbulence constitutes a contributing factor. Combining both theories leads to the conclusion that there is a threshold relationship between turbulence and fog formation (Zhou and Ferrier 2008). These methods are based on local scale parameters, but fog climate variation is also related to large scale environment change.

In Pakistan and northern India winter precipitation primarily results from eastward-propagating midlatitude cyclones from the Mediterranean region (Martyn 1992). These systems are often observed as closed cyclonic circulations at sea-level and are usually called Western Disturbances (WDs) (Pisharoty and Desai 1956). Precipitation is enhanced in the northern region due to blocking and upslope conditions imposed by the high mountain ranges of this region. WDs also cause precipitation over the northern plains of Pakistan and India. Once it rains, this inducts large amount of water vapor into the lower atmosphere by evaporation of precipitation. As soon as the low pressure passes, the leading edge of a high pressure system typically imposes clear and statically stable atmospheric conditions, leading to the formation of strong surface-based inversions. This enhances relative humidity close to the surface and facilitates fog formation. Badarinath et al. (2009) identified that when intense fog is observed over Indo-Gangetic (IG) region, the temperature anomaly at 700 hPa had higher values, and they attributed this to upper tropospheric heating due to absorption of solar irradiation, contributing to the enhanced stability of the lower troposphere. This region is highly influenced by black carbon (BC) during winter, which heats the lower free atmosphere by absorption of solar radiation. They also suggested the importance of transport of fog and aerosols from foggy regions dominated by agriculture crop-residue burning towards the southern peninsular region of India.

Watanabe (2004) showed by means of a simple linear regression analysis to observed monthly anomalies that the North Atlantic Oscillation (NAO) does have a wider horizontal scale. Watanabe (2004) also used a linear barotropic model and detected vorticity sources that effectively excite the Rossby waves and hence linked the NAO signal over the Atlantic with downstream circulation anomalies. The nearly hemispheric scale of the NAO is due to a downstream extension by a zonally oriented pattern in upper air circulation anomalies toward East Asia and the North Pacific. This appears the same as the circumglobal teleconnection described by Branstator (2002). Such a pattern in the monthly mean fields can be interpreted as quasi-stationary Rossby waves on the Asian jet waveguide (Hoskins and Ambrizzi 1993). Syed et al. (2006, 2010) linked the inter-annual variability in winter precipitation over northern Pakistan and India with El Niño/La Niña-Southern Oscillation (ENSO) and North Atlantic Oscillation (NAO). Yadav et al. (2009) also studied the NAO effect and found that the intensified Asian jet over North Africa to Middle East and the cascading down of the Rossby waves from the north Atlantic along the Asian jet effects the north western India winter precipitation. Li et al. (2008) showed the teleconnection pattern with a high-latitude path between NAO and the climate downstream of the Tibetan Plateau.

In this study we investigate the fog variability and trends over the last decades using both observation data and a detection scheme of fog based on different meteorological parameters of ERA-Interim reanalysis data, in order to explore inter-annual winter fog variability. Different empirical techniques are applied at airports to forecast fog but this large scale fog detection method has not been tested over south Asia. Reanalysis data from NCAR/NCEP reanalysis is also used to elucidate the reasons for inter-annual fog variability in the region of interest. The paper is organized with an overview of the data used in Sect. 2, the results are presented in Sect. 3 while the main results are summarized in Sect. 4.

2 Data

The meteorological data used in this study were obtained from the National Climatic Data Center (NCDC) of the National Oceanic and Atmospheric Administration (NOAA), based on data exchanged under the World Meteorological Organization (WMO) World Weather Watch Program. This data set provides daily meteorological records including the present weather code which describes weather phenomena such as fog, hail, thunder and other important types of weather. Some additional data for fog frequency were obtained from Pakistan Meteorological Department. Data from 82 sites, mostly located in urban areas, from 1976 to 2010 is used in this study. These stations report fog according to WMO definition, that fog is a suspension of very small droplets in the air that reduces surface visibility to less than 1 km (WMO 1992).

For examination of the characteristics of the large scale circulation, we have used monthly mean re-analysis data of National Centers for Environment Prediction NCEP/NCAR (Kalnay et al. 1996), as it provides the longest temporal overlap with the station data. This data has a horizontal resolution of 2.5° × 2.5° at standard pressure levels. For application of the fog detection scheme, we instead employ the European Centre for Medium-Range Weather Forecasts (ECMWF) reanalysis, ERA-Interim (Dee et al. 2011), 3 hourly surface and sigma level forecast data. ERA-Interim not only has a higher resolution than many other reanalysis products but also is improved in many other ways, especially using the 4D-Var data assimilation system. We use 03, 06 and 09 UTC forecasts initiated at 00 UTC, and 15, 18 and 21 UTC forecasts initiated at 12 UTC to allow a proper spin-up of moist processes and to enhance the temporal resolution. ERA-Interim was obtained from the ECMWF data server on a fixed grid of 1.0° × 1.0°. ERA-Interim monthly mean data is also used to investigate the regional variability of humidity and boundary layer stability.

3 Results and discussions

3.1 Fog climatology and trend

The December–January–February (DJF) mean (1976–2010) frequency of fog is shown in Fig. 1a, where fog frequency is defined from the number of days of fog divided by total number of days of available data in DJF. Fog frequency is high over a large area from Pakistan to Bangladesh across northern India from west to east, running almost parallel to south of Himalayas, roughly 3,000 km in the east–west and 500 km north–south extension. Choudhury et al. (2007) used satellite data to estimate that the maximum fog affected area in the winter of 2002–2003 was about 867,000 km^2. Fog events are sometimes observed to develop simultaneously over the vast region of the IG plains, easily detected in satellite morning visible imagery as large scale white patches of fog persist up to mid-day (Rajendra Kumar and Ajit 2010). The most favorable area for fog formation normally lies over western parts of the IG plain, covering Delhi, Punjab, Haryana and Uttar Pradesh where more than 18 % of all days have fog (Fig. 1a). The high frequency of fog results from high availability of moisture, coming either from moving western disturbances or vast irrigated agricultural fields, where abundant vegetation is sustained by irrigation. Low temperatures and

calm wind conditions over the region facilitate the persistence of fog for longer period.

Almost all of the stations with a mean fog frequency larger than 3 % display positive trends at the 99 % significance level (Fig. 1b). This yields a broad band of increasing fog occurrence along foothills of the Himalayas. Most of the stations show an increasing trend of more than 8 %-units per decade in the mean frequency of fog occurrence during winter. This means the fog frequency has increased more than 3 times over the last 30 years. Many other studies over different regions of the world have reported a decrease in fog occurrence frequency, particularly in recent decades, for instance in Germany (Sachweh and Koepke 1995), in US (Steve 2005). In China e.g. Shi et al. (2008) reported a decrease in fog frequency over Anhui province and linked it to the effect of the increasing urban heat island. On the other hand, Niu et al. (2009) showed a significant increase in the fog frequency over eastern-central China and linked it to the weakening of the East Asian monsoon circulation due to increased urban aerosol loading. The favorable local factors like moisture availability, radiative cooling, stability and also favorable large-scale meteorology seem to act in such a way as to increase the fog occurrence over northern India in contrast to some regions of China and elsewhere.

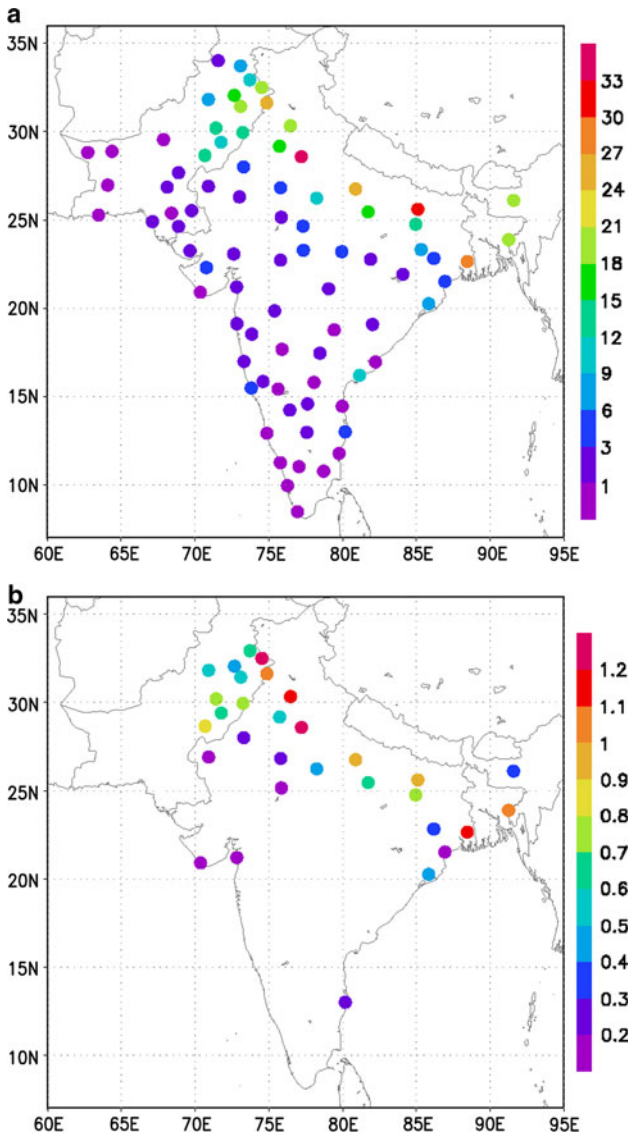

Fig. 1 **a** The mean frequency of fog (%) in winter (DJF) and **b** the annual rate (percentage per year) of changes in the mean frequency of fog during wintertime over south Asia at 82 sites from 1976 to 2010. In **b**, only stations with trends at the 1 % significance level are shown

To examine the spatial and temporal behavior of the fog variability we performed an Empirical Orthogonal Functions (EOF) analysis of fog frequency for all 82 stations. Figure 2 shows the first EOF (explained variance 58.5 %) and the related principal component (PC1). It is interesting to note that almost all the stations show positive values (Fig. 2a), indicating that fog variability is coupled over the whole region on the inter-annual time scale. Therefore, it seems reasonable to assume that the inter-annual variability is governed by some large scale phenomenon. PC1 shows significant trends and shifts in the occurrence of fog (Fig. 2b). We also performed the EOF analysis on the detrended fog frequency data (not shown); the first EOF and its principle component showed very similar inter-annual variability, except that the explained variance was reduced to 38.5 %.

3.2 Regime shifts in the fog frequency

The time series of the average fog frequency is shown in Fig. 3a, using 31 stations with a significant trend at the 1 % level from 1976 to 2010. The increase in the fog frequency is not gradual but instead shows large step-like changes at distinct times. Therefore, we apply a regime shift indicator test (Rodionov 2004) on the mean frequency of occurrence. This test is based on the sequential *t* test analysis of regime shifts. The user-defined parameters for the test are the target significance level, the cut-off length, and the Huber weight parameter. In this analysis a significance corresponding to the p-level 0.01 is selected. The cut-off length is taken as 10 years, which is similar to the cutoff length in filtering and affects the time scale of the regimes by discounting regimes of shorter length. The Huber weight parameter is set to 2, which affects the treatment of outliers by weighing them inversely proportional to their distance from the mean value of the regime. With these parameters, the method utilizes a sequential approach to determine the timing of regime shifts. The identification of a regime shift is based on calculating the regime shift index (RSI, see Rodionov 2004). Briefly it represents a cumulative sum of normalized deviations of the time-series values from the

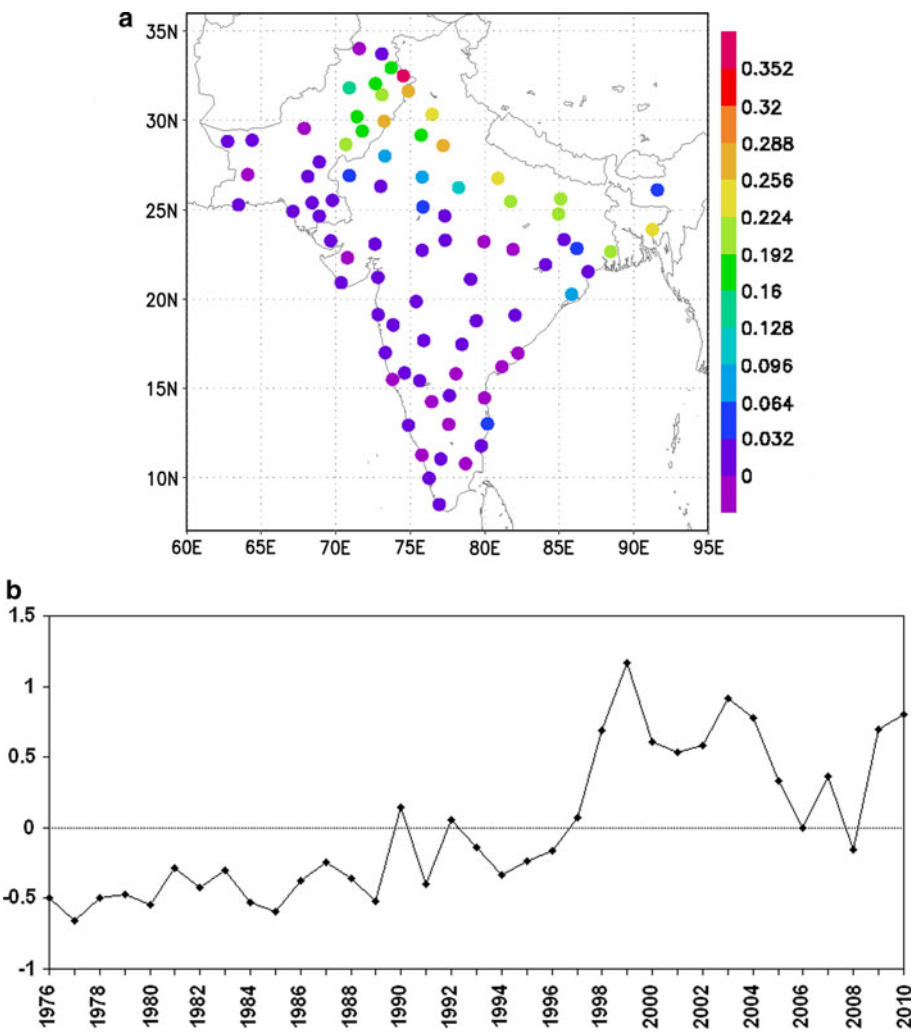

Fig. 2 **a** First EOF of DJF (1976–2010) fog frequency and **b** the corresponding PC

hypothetical mean for the new regime. This is the level for which the difference to the mean for the previous regime is statistically significant according to Student's *t* test. If the RSI remains positive during a time period equal to the cut-off length, a regime shift is determined.

Three regimes are identified; Regime-1 (1976–1989) with a mean fog fraction of 6.1 %, Regime-2 (1990–1997) with a mean fog fraction of 10.1 % and Regime-3 (1998–2010) with a mean fog fraction of 19.5 % (Fig. 3a). The shift from Regime-2 to Regime-3 has the largest magnitude of jump, not only in mean but also in the variance. The analysis of some of the stations for which the data are available also before 1976 revealed a fog fraction below 7 % (not shown), i.e. the system was in Regime-1 also before 1976. We also applied this regime shift analysis to individual stations in order to identify the year in which each station shows a significant change in the mean and variance of the fog occurrence. Figure 3b shows that maximum number of stations displays the shift in 1990 and 1998. For a few stations the method also detected an additional shift in 2005 due to a relatively low fog frequency in 2006 and 2008.

3.3 Inter-annual variability and the large scale dynamics

Correlations between the detrended PC1 of observed fog (hereafter called Fog Index) and 300 hPa geopotential heights in the Northern Hemisphere winter (DJF) from 1976 to 2010 show a wave train from northern Europe to eastern India (Fig. 4a). Similar correlations for 700 hPa geopotential heights are shown in Fig. 4b. The wave train seems to be barotropic, with positive geopotential anomalies over the northern parts of South Asia associated with the higher fog frequency. These high-pressure anomalies over the region from lower to upper troposphere can contribute to stable conditions and hence cause favorable conditions for the formation of fog.

Branstator (2002) found a circumglobal teleconnection in the northern hemisphere winter and identified that the

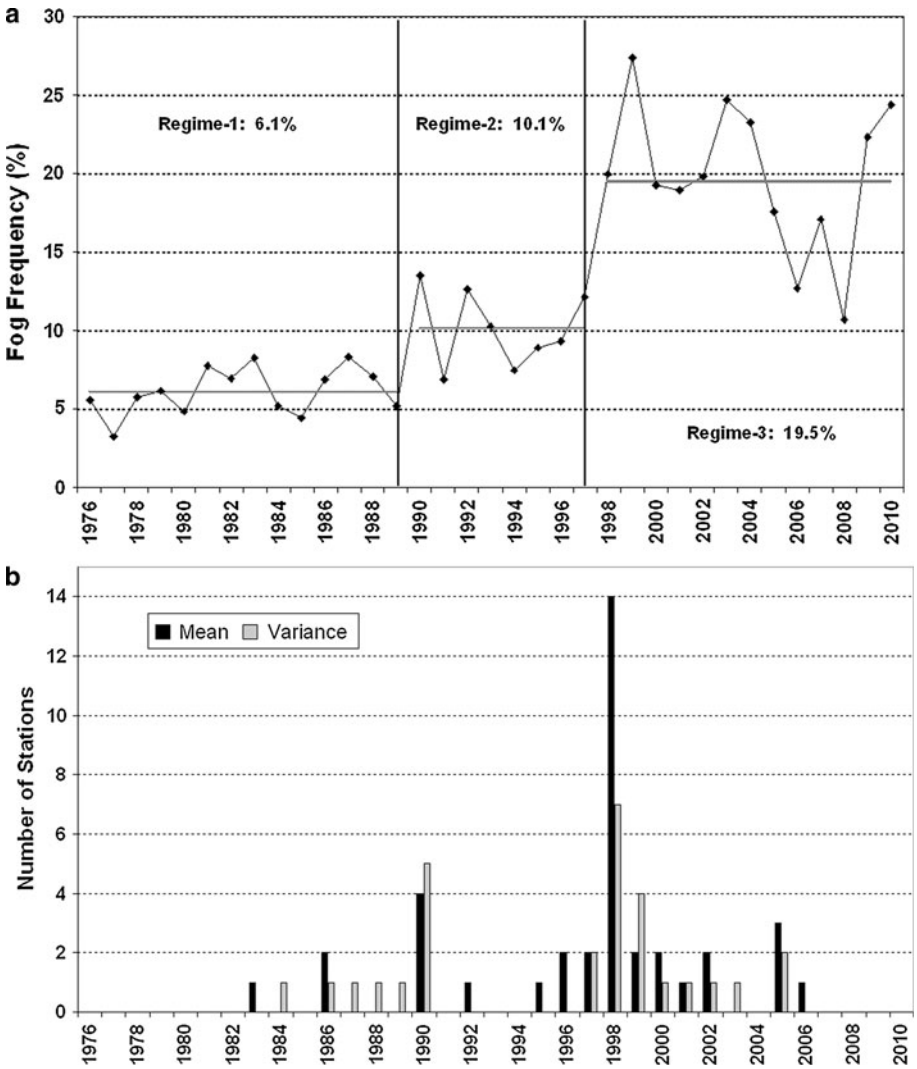

Fig. 3 **a** Time series (1976–2010) of the average percentage of fog frequency of all the stations which have significant trend in the fog frequency. **b** The year in which each station show shift in regime at 1 % significance level with respect to mean and variance

nearly hemispheric scale of the NAO is due to a downstream extension toward East Asia and the North Pacific by a zonally oriented pattern in the upper air circulation anomalies. Such a pattern in the monthly mean fields can be interpreted as quasi-stationary Rossby waves on the Asian jet waveguide (Hoskins and Ambrizzi 1993). The anomaly is most clearly seen on interannual time scales in the meridional wind anomaly, which shows a wavetrain along the Asian jet with an anomalous vorticity source near the jet entrance (Watanabe 2004). Interannual variability of the NAO is also tied to the East Asian climate variability such that a positive NAO tends to bring a surface warming over East Asia (Watanabe 2004). Branstator (2002) found that there exist a family of waveguide patterns, i.e. some points in the South Asian waveguide have more distant teleconnections than do others. Moreover, disturbances that are trapped in the South Asian jet stream waveguide do not have preferred longitudinal phases within the waveguide and are composed primarily of zonal wave-number 5. The anomalous meridional wind is a better indicator of the NAO downstream extension than geopotential heights, as we are interested in behavior in the vicinity of the South Asian mean jet and do not wish to use a field whose variance is diminished at low latitudes. Therefore, we also performed the correlation analysis between the Fog Index and the 300 hPa meridional winds. As the largest shift in the fog frequency with respect to mean and variance is observed in 1998, we perform the correlation analysis for the periods 1976–1997 (22 years) and 1998–2010 (13 years). This also indicates that variability in this region is largely trapped in the jet and consists of a pattern that covers a broad longitudinal domain, almost circumscribing the whole globe, especially for the first period 1976–1997 (Fig. 4c). For the period 1997–2010, the wave-train seems to split into two patterns (Fig. 4d), one propagating from the south of the Mediterranean Sea and the other over northern Europe. However, the patterns over South Asia are very similar for both the periods.

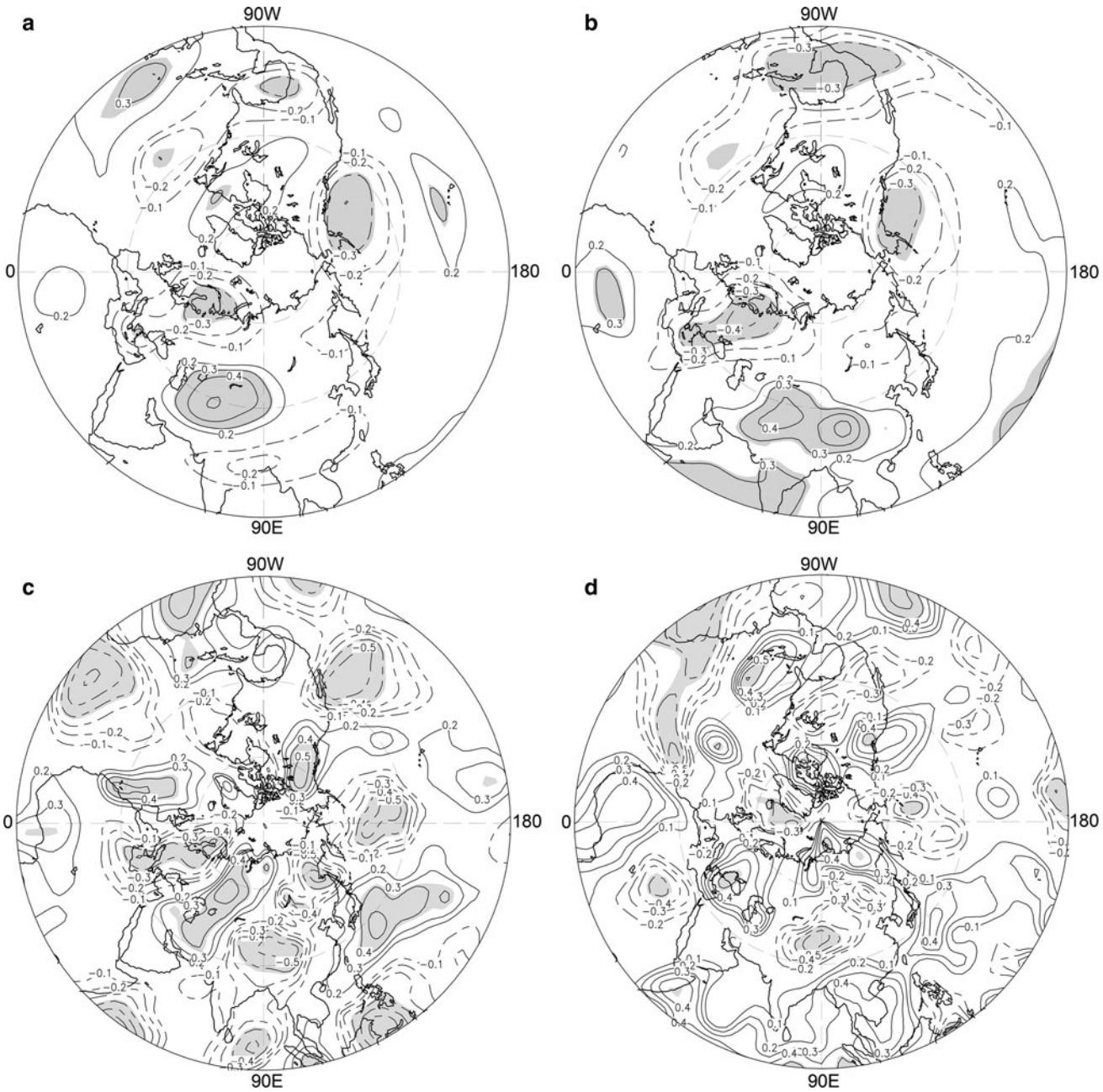

Fig. 4 Correlation between Fog Index and the northern hemisphere mean DJF **a** 300 hPa geopotential heights (1976–2010), **b** 700 hPa geopotential heights (1976–2010), **c** the 300 hPa meridional winds (1976–1997), **d** the 300 hPa meridional winds (1998–2010), regions where correlations are statistically significant at the 5 % level are *shaded*

The composites of different regimes for the difference with the mean do not show significant changes in the large scale circulation and also the wave train activity does not seem to have any trends. To study the temporal variations in the wave train activity we calculated the index following Li et al. (2008) by taking values of geopotential at the cores of nodes and antinodes of the wave train and we found no significant trend in the wave train activity (not shown). Therefore, in the next sections we focus more on the regional scale.

3.4 Fog detection and variability in ERA-Interim reanalysis data

ERA-Interim reanalysis data is only available from 1979 to present, but at a higher resolution; therefore we used this data to detected fog to investigate the local variability of some of the parameters associated with fog, e.g. humidity and boundary-layer stability. Direct usage of the lowest-level clouds as a fog estimator (Teixeira 1999) was tested

for the ERA-Interim data, but the result did not show the observed behavior (Fig. 3a). Therefore, a fog detection scheme is instead employed.

3.4.1 Fog detection scheme

Our motivation to detect fog in the ERA-Interim forecast data is not for forecasting per se, but to investigate the variability of fog over the region in the reanalysis data. Nevertheless, the results here can be interpreted as in indication of the capability of the applied method in conjunction with the ECMWF model to capture fog events over this region. However, we will not explore this aspect further in this paper.

As long as the specific humidity decreases with height, radiation fog usually does not form, except in still air and even then the cooling may result only in dew or rime on the ground (Petterssen 1940). Therefore, we adopted the Baker et al. (2002) concept of a "crossover temperature (Tx)" for radiation fog formation. The crossover temperature Tx is defined as the minimum dew point observed during the warmest hours in the preceding afternoon, assuming no other influence. Fog is assumed to form when the near-surface air temperature reaches or falls below Tx, rather than below the dew point. This can be understood from the following argument. Under normal atmospheric conditions, specific humidity decreases with height and in a well-mixed boundary layer the surface dew point will decrease during the warmest hours of the day because the turbulent flux of water vapor is directed away from the surface. After the warmest hours have passed, the near-surface dew point will rise a few degrees as the upward moisture flux ceases and evaporated moisture is trapped in a more shallow layer. During the night the temperature will fall and at some time become equal to the dew point (saturation). As long as the flux of water vapor is still directed upward, the temperature and dew point will continue to fall together without forming fog as long as the specific humidity decreases with height. As the air continues to cool, the water–vapor flux eventually reverses direction; this happens when T = Tx, and when the temperature falls below Tx, fog may begin to form.

For radiation fog forecasting, just knowing the vertical moisture profile is not sufficient. If the lower boundary layer is sufficiently turbulent, vertical mixing can cause the fog to lift and instead form a low stratus clouds. Therefore, MRi is used to account for the effects of turbulence. Formation, development and dissipation of this type of fog strongly depend on the levels of near-surface turbulence and using the MRi is one way to account for this process. A high Richardson number indicates that the lower troposphere air flow is decoupled from the air flow at the surface, thus turbulence at the surface is low and fog formation is more likely. A low Richardson number indicates the surface air flow is coupled with the lower troposphere airflow, thus turbulence is greater and low stratus clouds are more likely. This discussion is limited to radiation fog, and is not necessarily valid when advection is involved. Advection involving air with dew points in excess of about 6° C higher than the underlying surface temperature can lead to fog formation also in well mixed boundary layers; for these situations MRi is irrelevant (Baker et al. 2002). This type of fog can develop at any time when such advection conditions prevail and last for several hours.

There are, however, other ways to account for these processes. According to a recent study by Zhou and Ferrier (2008), one can define a so-called "critical turbulence exchange coefficient", Kc, for every radiation fog, where Kc is an explicit function of temperature, pressure, cooling rate (Cr) and depth of saturated layer (or fog depth, Hs) near the surface, and they suggest that $Kc \sim Cr^{1/2}$ and $Hs^{3/2}$; Kc is also proportional to temperature. The condition for formation, or persistence, of radiation fog was found to be $K < Kc$, where K is actual turbulent exchange coefficient, estimated as a function of the Richardson number. Thus, the turbulence threshold for radiation fog is not fixed but depends on the specific situation. For example, if the air temperature is higher, the saturated layer near the surface is deeper, or cooling rate is larger, fog is more likely to form because of larger Kc. On the other hand, if temperature, cooling rate and turbulence are same, but the saturated layer is shallow, fog may not form. As an initial test of the concept we use the Baker et al. (2002) approach for simplicity, but Zhou and Ferrier's theory still can be used in our discussion. The value of MRi can be calculated as follows.

$$\mathrm{MRi} = (T_b - T_{sfc})/U^2 \quad (1)$$

Here T_b is the boundary layer temperature (°C), T_{sfc} the near surface temperature (°C) and U the boundary layer wind speed (knots).

We use the temperatures and wind speeds from the ERA-Interim sigma-level data at an approximate height of 30 m to represent the boundary layer values, whereas the near-surface temperature is taken at the lowest sigma level, at ~10 m height. Figure 5a shows the detected mean (1990–2010) frequency of fog fraction in winter, using the method described above. Fog is detected only over the regions with elevation less than 1,000 m. Three hourly ERA-Interim forecast data is used to detect fog events at each grid point. The thresholds $0.15 \leq \mathrm{MRi} \leq 0.8$ were adopted after some testing; the upper threshold is only used because on a very few days and only a few grid points, very high spurious MRi values were detected because of large vertical temperature differences combined with very low winds (see equation). The spatial and temporal structure of

detected fog is not very sensitive to the choice of the MRi thresholds, but the magnitude of the detected fog varies with changes in these values. The spatial pattern and the magnitude of fog occurrence (Fig. 5a) are very well detected comparing to the observations (Fig. 1a).

The EOF analysis of the diagnosed fog shows some interesting features. The fog variability on inter-annual time scale is coupled over South Asia, as in observations, but not over Burma. The corresponding PC1 (Fig. 3a) shows the intermediate level variance in the fog variability from 1990 to 1997, matching well with Regime-2 in the observations. For a high variance regime after 1997, which corresponds well with the observed Regime-3, however, the variance during 1980 s is higher compared to Regime-1 in the observations (Note that the use of ERA-Interim precludes analysis before 1979.). The correlation between the PC1 of the diagnosed fog and Fog Index from observations is 0.7. The high peaks at 1999 and 2004 and a plateau between these peaks is also very well captured, compared to observations. However, at a few of the years, the inter-annual variability is not well detected. Keeping in mind that only radiation fog is detected by this method and that the same thresholds of MRi are applied over a very large domain and for all different conditions, the results are still very encouraging.

3.4.2 *Changes in the boundary layer over south Asia*

Dai (2006) found that although global changes in surface relative humidity (RH) are generally small, RH may increase substantially on regional scales. For example, Dai (2006) showed a significant increase (0.5–2.0 % per decade) over central and eastern United States, India, and western China, accompanied with large upward trends in

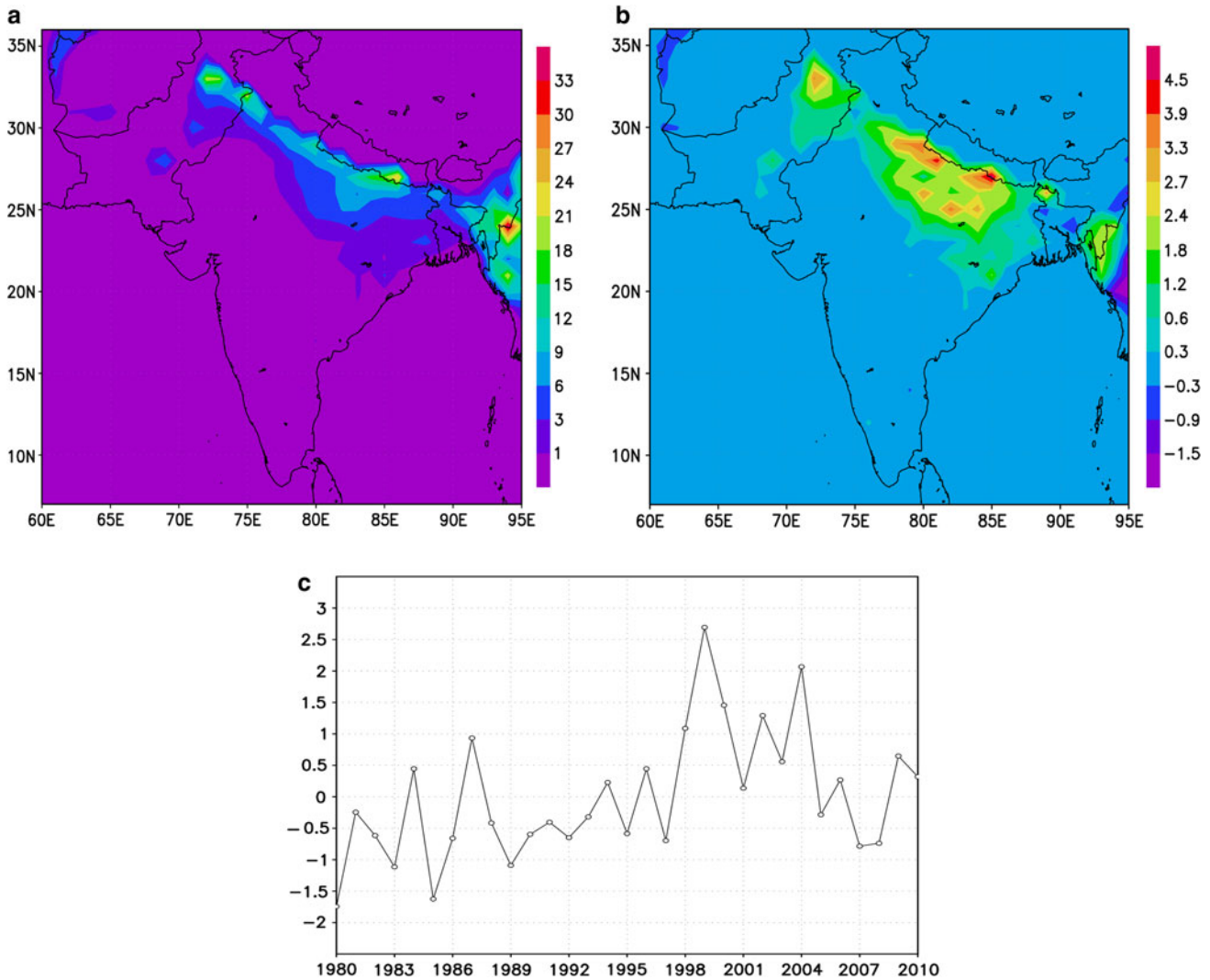

Fig. 5 **a** The detected mean frequency of fog (%) in winter (DJF), **b** the first EOF of mean DJF fog frequency and **c** its corresponding PC for 1980–2010

surface specific humidity and total cloud cover. The strong correlation between near-surface specific humidity and temperature on both interannual and longer time scales (including the trends) suggests that the increasing trends in global specific humidity will continue as global temperature rises. However, increasing temperatures may also lead to a reduction in the night-time cooling reducing radiation fog formation. Global warming leads to drop in night cooling, but increase in RH usually leads to deeper RH depth near the ground. According to $Kc \sim Cr^{1/2}$ and $Hs^{3/2}$ (Zhou and Ferrier 2008), RH depth (Hs) has a much larger impact on Kc than cooling rate (Cr) does (3/2 vs. 1/2). Therefore, increasing RH near the ground is more likely to raise Kc, which is favorable for fog formation and persistence. The winter precipitation from WDs over Pakistan and northern India does not show a significant trend and the inter-annual variability of precipitation is also not correlated with the fog variability.

The composite difference 1998–2006 minus 1985–1997, in winter mean relative humidity at 1,000 hPa is shown in

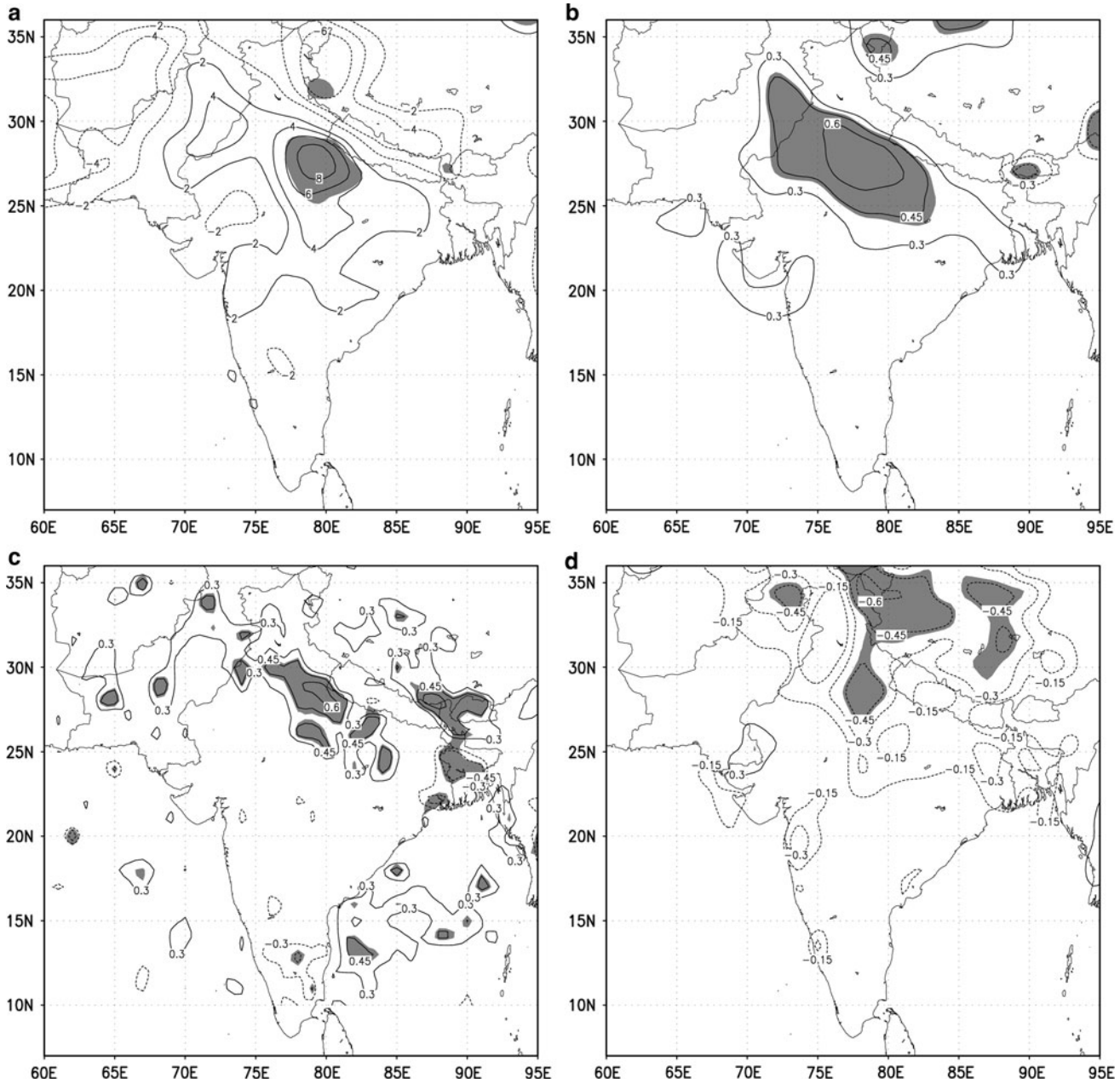

Fig. 6 **a** Composite difference (1998–2010) minus (1985–1997) for the mean winter (DJF) relative humidity at 1,000 hPa and the correlation (1976–2010) of detrended PC1 of fog frequency with **b** relative humidity, **c** the Modified Richardson number (MRi), and **d** boundary layer height. Regions where the difference and correlation is statistically significant at the 5 % level are *shaded*

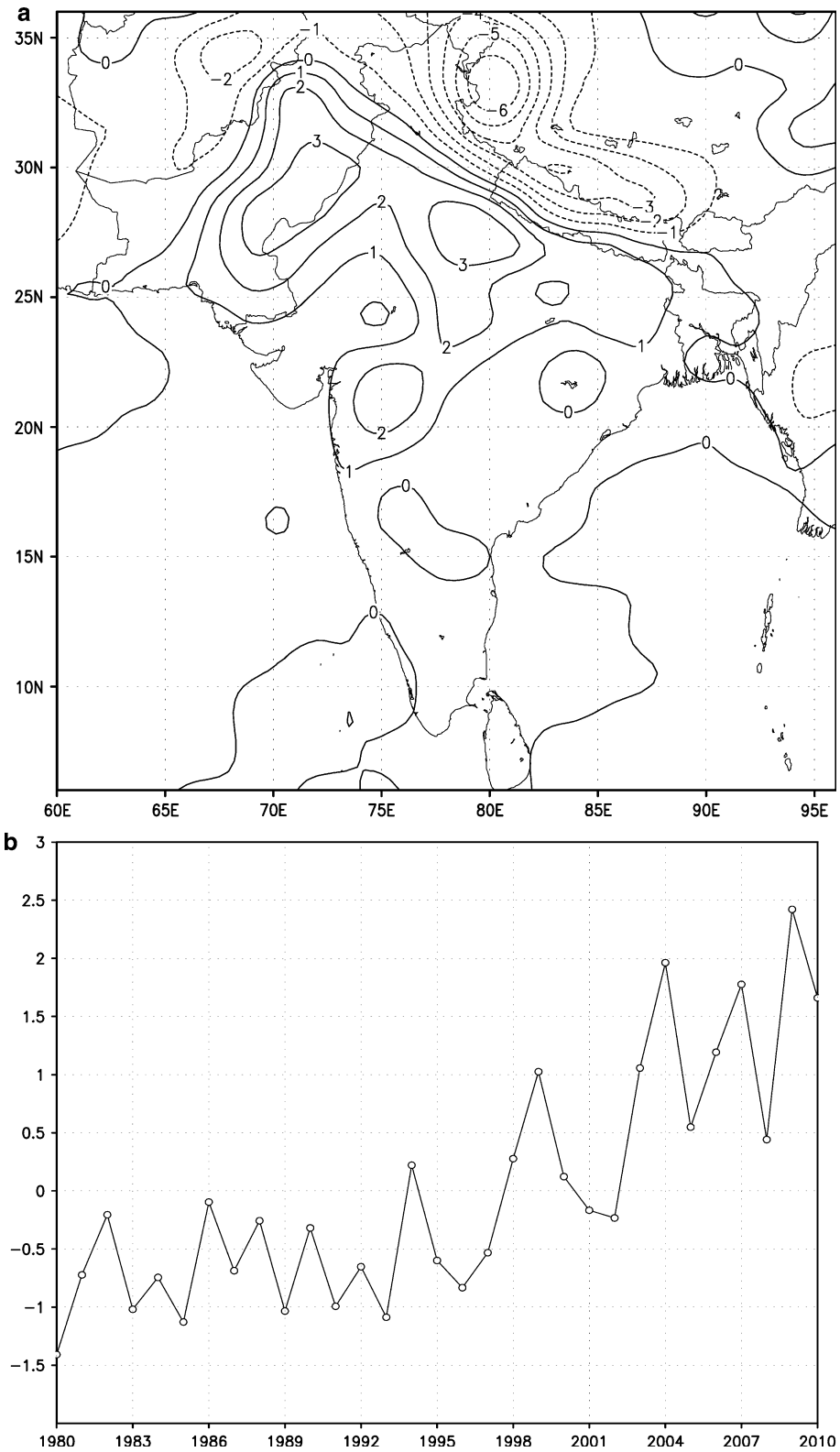

Fig. 7 **a** Third EOF of mean DJF (1990–2010) relative humidity at 1,000 hPa in winter (DJF) and **b** the corresponding PC

Fig. 6a. A significant increase in RH can be seen over IG plains; a similar increase is also found in specific humidity (not shown). The results are consistent with the study of Jaswal and Koppar (2010), in which they used station data all over India and found trends up to 4.96 % per decade in RH from 1969 to 2007 over the IG plains. The Fog Index is highly correlated with RH over IG the plains (Fig. 6b), and the correlation with MRi and boundary layer height

(Fig. 6c, d) shows that the increase in the fog and RH is accompanied with a decrease in boundary layer height and an increase in the stability of the boundary layer. These changes in the boundary layer are consistent with the presence of higher pressure over the region as discussed in Sect. 3.3.

The third EOF of the RH over south Asia (Fig. 7a, explained variance 11.5 %) seems to be related to the trend; it has a strikingly similar pattern to the composite difference (Fig. 6c), and the corresponding PC3 shows large inter-annual variability but a gradual trend in the RH. The trend in the PC3 is very similar to the actual time series of the RH over the region (not shown). The correlation between the PC3 of RH (Fig. 7b) with Fog Index is 0.73, significant at the 1 % level. PC3 does not show any trend in the 1980s, corresponding to Regime-1, but from early 1990s and onwards there is significant increasing trend.

4 Summary

The spatial and the temporal variation in fog frequency is investigated, using the observational station data in the South Asian region. Fog covers an extensive area, approximately 3,000 km from Pakistan to Bangladesh across north India from west to east running parallel to the foot hills of the Himalayas. The fog variability over the whole region is coupled and therefore likely governed by some large scale phenomenon on the inter-annual time scale. A downstream extension of the NAO, accomplished by quasi-stationary Rossby waves trapped on the Asian jet waveguide excited by a vorticity source associated with the NAO, facilitates stable atmospheric conditions conducive for the fog formation over the region. Significant increasing trends are found in the fog frequencies. The mean fog frequency has increased more than 3 times in the last 35 years and this increase shows different regimes with respect to both mean and variance. We detect the fog in ERA-Interim 3 hourly, surface and model level forecast data, using the concept of cross over temperature and boundary layer stability, and show that the method can be applied to detect fog over south Asia and thus can be used in fog forecasting. Gradual increasing trends are also found in specific and relative humidity over the region which is highly correlated with observed and detected fog.

We were unable to explain the sudden shifts in the regimes, neither with increasing humidity nor with the large scale dynamics, which govern the inter-annual variability of fog frequency. Being a multidisciplinary and multiscale problem, sudden shifts in the fog regimes may result from combinations of changes in local factors, like land use (e.g. cropping patterns, irrigation) and the role of aerosols etc., and a gradual increase in the RH (due to increasing global temperatures), and changes in the large scale circulation. There is evidence that atmospheric aerosols can be responsible for accelerating and intensifying the fog formation in urban areas (Mircea et al. 2002), which could be due to both direct and indirect effects of aerosols.

Acknowledgments Discussions with Saeed Falahat, Abdel Hannachi and Ian Simmonds are highly appreciated. F. S. Syed thanks the Higher Education Commission of Pakistan for financial support. We thank both reviewers for their very useful comments and suggestions.

References

Badarinath KVS, Shailesh Kumar K, Anu Rani S, Roy PS (2009) Fog over Indo-Gangetic plains—a study using multisatellite data and ground observations. IEEE J Select Topics Appl Earth Observat Remote Sens 2:3

Baker RJ, Cramer, Peters J (2002) Radiation fog: UPS Airlines conceptual models and forecast methods. In: 10th conference on aviation, range, and aerospace, Portland, OR, American Meteorological Society 5.11 (Available online at http://ams.confex.com/ams/pdfpapers/39165.pdf) (preprint)

Branstator G (2002) Circumglobal teleconnections, the jet stream waveguide, and the North Atlantic Oscillation. J Clim 15:1893–1910

Burrows WR, Garry Toth (2011) Automated fog and stratus forecasts from the Canadian RDPS operational NWP model. In: 24th Conference on weather analysis and forecasting. AMS, Seattle, Washington, USA, 23–27 January 2011

Choudhury S, Rajpala H, Sarafa AK, Panda S (2007) Mapping and forecasting of North Indian winter fog: an application of spatial technologies. Int J Remote Sens 28:3649–3663

Collier CG (1970) Fog at Manchester. Weather 25:25–29

Dai A (2006) Recent climatology, variability, and trends in global surface humidity. J Clim 19:3589–3606

Dee DP, Uppala SM, Simmons AJ et al (2011) The ERA-Interim reanalysis: configuration and performance of the data assimilation system. Q J R Meteorol Soc 137:553–597

Dutta HN (2010) Acoustic sounding probing of fog dynamics, forecaster-users interactive workshop on fog monitoring and forecasting services 2010–2011 Dec, 2010

Duynkerke PG (1999) Turbulence, radiation and fog in Dutch stable boundary layers. Bound-Layer Meteor 90:447–477

Fabbian D, Richard D, Stephen L (2007) Application of artificial neural network forecasts to Predict Fog at Canberra international airport. Weather Forecast 22:372–381

Fitzjarrald DR, Lala GG (1989) Hudson Valley fog environments. J. Appl. Meteor. 28:1303–1328

Gultepe I, Pagowski M, Reid J (2007) Using surface data to validate a satellite based fog detection scheme. Weather Forecast 22:444–456

Hoskins BJ, Ambrizzi T (1993) Rossby wave propagation on a realistic longitudinally varying flow. J Atmos Sci 50:1661–1671

Jaswal AK, Koppar AL (2010) Recent climatology and trends in surface humidity over India for 1969–2007. Mausam 62(2):145–162

Kalnay E et al (1996) The NCEP/NCAR 40-year reanalysis project. Bull Am Meteorol Soc 77:437–471

Koziara MC, Robert JR, Thompson WJ (1983) Estimating marine fog probability using a model output statistics scheme. Mon Weather Rev 111:2333–2340

Landsberg H (1964) Physical climatology, 2nd edn. Gray Printing, Dubois

Li J, Rucong Y, Zhou T (2008) Teleconnection between NAO and climate downstream of the Tibetan Plateau. J Clim 21:4680–4690

Martyn D (1992) Climates of the world. Elsevier, Amsterdam, 1st edn, p 436

Marzban C, Leyton S, Colman B (2007) Ceiling and visibility forecasts via neural networks. Weather Forecast 22:466–479

Mircea M, Facchini MC, Decesari S, Fuzzi S, Charlson RJ (2002) The influence of the organic aerosol component on CCN super saturation spectra for different aerosol types. Tellus B 54:74–81

Niu S, Lu C, Yu H, Zhao L, Lu J (2009) Fog research in China: an overview. Adv Atmos Sci 27(3):639–662. doi:10.1007/s00376-009-8174-8

Petterssen S (1940) Weather analysis and forecasting. McGraw-Hill, New York

Pisharoty PR, Desai BN (1956) Western disturbances and Indian weather. Indian J Meteorol 8:333–338

Rajendra Kumar J, Ajit T (2010) Spatial and temporal variation of Fog over Indo-Gangetic plains using IMD-IAF current weather available since 1980 s and Satellite data available since 1990s. Forecaster-Users interactive Workshop on Fog Monitoring and Forecasting Services 2010–2011, Dec 2010

Roach WT, Brown R, Caughey SJ, Garland JA, Reading CJ (1976) The physics of radiation fog I—a field study. Q J R Meteor Soc 102:313–333

Rodionov SN (2004) A sequential algorithm for testing climate regime shifts. Geophys Res Lett 31:L09204. doi:10.1029/2004GL019448

Rosenburg NJ, Blad BL, Verma SB (1983) Microclimate. Wiley, New York

Sachweh M, Koepke P (1995) Radiation fog and urban climate. Geophys Res Lett 22:1073–1076. doi:10.1029/95GL00907

Shi C, Roth M, Zhang H, Li Z (2008) Impacts of urbanization on long-term fog variation in Anhui Province, China. Atmos Environ 42:8484–8492

Steve L (2005) The disapperance of dence fog in Los Angles: another urban impact? Phys Geograph 26(3):177–191

Stoelinga MT, Warner T (1999) Nonhydrostatic, mesobeta-scale model simulations of cloud and visibility for an east coast winter precipitation event. J Appl Met 38:385–404

Syed FS, Giorgi F, Pal JS, King MP (2006) Effect of remote forcings on the winter precipitation of central southwest Asia part 1: observations. Theor Appl Climatol 86:147–160

Syed FS, Giorgi F, Pal JS, Keay K (2010) Regional climate model simulation of winter climate over Central-Southwest Asia, with emphasis on NAO and ENSO effects. Int J Climatol 30:220–235. doi:10.1002/joc.1887

Tardif R (2007) The impact of vertical resolution in the explicit numerical forecasting of radiation fog: a case study. Pure Appl Geophys 164:1221–1240

Teixeira J (1999) Simulation of Fog with the ECMWF Prognostic cloud scheme. Q J R Meteor Soc 125-B:529–553

Terradellas E, Ferreres E, Soler MR (2008) Analysis of turbulence in fog episodes. Adv Sci Res 2:31–34

Tiwari S, Payra S, Bisht DS (2010) Visibility degradation during foggy period due to anthropogenic Urban Aerosol at Delhi, India 5th International Conference on Fog, Fog Collection and Dew, 25–30 July, 2010, Münster, Germany. http://www.fogconference.org,id.FOGDEW2010-48

Toon OB, Tabazadeh A, Browell EV, Jordan J (2000) Analysis of lidar observations of Arctic polar stratospheric clouds during January 1989. J Geophys Res 105:20589–20615

Turton JD, Brown R (1987) A comparison of a numerical model of radiation fog with detailed observations. Q J R Meteorol Soc 113:37–54. doi:10.1002/qj.49711347504

Watanabe M (2004) Asian jet waveguide and a downstream extension of the North Atlantic Oscillation. J Clim 17:4674–4691

Welch RM, Welicki BA (1986) The stratocumulus nature of fog. J Appl Meteorol 25:101–111

WMO (1992) International meteorological vocabulary, WMO 182, p 782

Zhou B, Du J (2010) Fog prediction from a multimodel mesoscale ensemble prediction system. Weather Forecast 25:303–322

Zhou B, Ferrier BS (2008) Asymptotic analysis of equilibrium in radiation fog. J Appl Meteor Clim 47:1704–1722